Effective control of filament efficiency by means of spacer HfAlO$_x$ layers and growth temperature in HfO$_2$ based ReRAM devices

G. Vinuesa[a], Ó. G. Ossorio[a], H. García[a], B. Sahelices[a], H. Castán[a], S. Dueñas[a,*], M. Kull[b], A. Tarre[b], T. Jõgiaas[b], A. Tamm[b], A. Kasikov[b], K. Kukli[b]

[a]*Department of Electronics, University of Valladolid, Paseo de Belén 15, Valladolid, E-47011, Spain*
[b]*Institute of Physics, University of Tartu, W. Ostwald 1, Tartu, 50411, Estonia*

Abstract

Resistive switching random access memories are being thoroughly studied as prospective non-volatile memories. In this paper, we report electrical characterization of HfO$_2$-Al$_2$O$_3$ based metal-insulator-metal structures devised using atomic layer deposition. Dependences of electrical behavior on HfO$_2$:Al$_2$O$_3$ cycle ratio is studied. An explanation for the differences between the Resistive Switching properties of the samples is proposed, based on the distribution of HfAlO$_x$ layers of the sample. Dependence of the RS properties of the samples on their growth temperature is discussed.

Keywords: RRAM, NVM, MIM stack, resistive switching, hafnium oxide, aluminium oxide, alumina, hafnium-aluminum oxide

1. Introduction

Non-volatile memory devices based on the resistive switching (RS) effect are considered as the most promising technology for future memory applications due to their excellent characteristics, such as good dimensional scalability and small operating voltages. The RS effect is based in the growth of conductive filaments (CF) in the dielectric film mounted between metal electrodes under a voltage applied to the electrodes [1, 2]. While HfO$_2$ is one of the most widely studied dielectrics for the fabrication of ReRAM devices [3], alternately layered nanomaterials are of increasing interest [4], as screening of the most appropriate combinations of materials for the dielectric layer is one of the issues in ReRAM fabrication.

In several previously conducted works, HfO$_2$-Al$_2$O$_3$ films have demonstrated advanced RS characteristics in comparison with both single HfO$_2$ and Al$_2$O$_3$ films. Resistive switching behavior has been evaluated in Al$_2$O$_3$/HfO$_2$ bilayer [5, 6, 7], Al$_2$O$_3$/HfO$_2$/Al$_2$O$_3$ trilayer [4, 7], and pentalayer [7] structures ALD-grown at 225 - 250 ℃ with total thicknesses reaching 20 nm. In another study, Al$_2$O$_3$/HfO$_2$/Al$_2$O$_3$ trilayers grown at 150 ℃ with thicknesses of 12 nm were able to demonstrate multilevel switching characteristics [8]. Periodical HfO$_2$-Al$_2$O$_3$ multilayers containing equal amounts of Hf and Al have been grown to a thickness of 6.5 nm at 250 ℃ [9]. However, in this latter study the thickness of the constituent layers was not revealed. Hf$_x$Al$_{1-x}$O$_y$ films have been grown at 240 ℃ with graded profile whereby the HfO$_2$:Al$_2$O$_3$ ALD cycle ratio was varied from 9:1 to 1:4 [10]. Another study indicated that 30 nm thick nanolaminates of HfO$_2$-Al$_2$O$_3$ bilayers composed of 1.2 nm thick HfO$_2$ and 0.2 nm thick Al$_2$O$_3$ layers could be grown at temperatures as low as 100 ℃ [11].

The application of 3 consecutive HfO$_2$ ALD cycles alternately with 2 Al$_2$O$_3$ cycles has enabled the deposition of RS-behaving HfO$_2$-Al$_2$O$_3$ multilayers at 200 ℃ with total thicknesses of 8 nm, showing an improvement in the High Resistance State (HRS) retention characteristics when compared with HfO$_2$-only films [12]. In the latter study, however, the precursor chemistry was not revealed. Apparently, contradicting results were obtained in a study, where HfO$_2$ films doped with 7 at.% Al were grown using HfO$_2$:Al$_2$O$_3$ ALD cycle ratio of 12:1 to the thickness of 5-6 nm from Al(CH$_3$)$_3$, (MeCp)2Hf(Me)(OMe) and H$_2$O at 300 ℃ [13]. In the latter study, filament disruption was, as proposed, suppressed by the defects introduced by Al$_2$O$_3$ as the high resistance state was stabilized at higher currents. Most commonly, the metal precursors exploited in ALD of resistively switching stacks consisting of HfO$_2$ and Al$_2$O$_3$ have been Hf[N(C$_2$H$_5$)CH$_3$]$_4$ (TEMAHf), and Al(CH$_3$)$_3$ (TMA), whereby H$_2$O served as oxygen precursor [4, 5, 6, 7, 8, 9, 10, 11].

The present study is devoted to the resistive switching properties of HfO$_2$-Al$_2$O$_3$ multilayers, whereby the films were grown by ALD to thicknesses of 10-15 nm at different temperatures of 300 ℃ and 400 ℃ from TEMAHf, TMA, and O$_2$ plasma. Examination of differences in the properties of the selected films grown using different periodicity of constituent oxides and at different growth temperatures was of importance.

2. Experimental details

Atomic layer deposition of HfO$_2$–Al$_2$O$_3$ multilayer films was carried out using TEMAHf, TMA and remote O$_2$ plasma in a commercial Picosun TM R-200 Advanced ALD system.

---

*Corresponding author
Email address: sduenas@ele.uva.es (S. Dueñas)

TEMAHf and TMA were evaporated at 100ºC and 22 ºC, respectively. The amorphous films were grown on TiN/Si substrates by changing the HfO_2:Al_2O_3 cycle ratio between 1:1 and 9:1 with a total amount of 100 ALD cycles to the thickness of 12-16 nm, somewhat influenced by the cycle ratios. All the samples were supplied by top Ti electrodes with an area of 0.052 mm^2, by electron-beam evaporation through shadow mask at room temperature. Since a single ALD cycle of Al_2O_3 can, plausibly, not result in the formation of a full oxide mono-layer, the solid multilayers grown in such experiments may also be regarded as HfO_2 films deposited alternately with some-what diffuse $HfAlO_x$ barrier layers (which can be referred to as spacer layers). The host HfO_2 films were grown using ALD cycle sequence of 0.3-4.0-15.0-4.0 seconds for TEMAHf pulse-purge-O_2 plasma pulse-purge times respectively. The intermediate Al_2O_3 cycle followed a sequence of 0.1-4.0-15.0-4.0 seconds applied for TMA pulse-purge-O_2 plasma pulse-purge times. Sample series with HfO_2:Al_2O_3 cycle ratios 1:1, 4:1 and 9:1 was grown at 300ºC, completed with a film grown with the cycle ratio of 9:1 at 400 ºC. The list of samples with their respective characteristics can be found in Table. I.

Sample	T_{GROWTH}	Cycle Sequence	HfO_2:Al_2O_3 cycle ratio	Al:Hf ratio	Thickness	n
H1A1	300 ºC	$50 \times [1 + 1]$	1:1	0.96	19.2 nm	1.49
H4A1	300 ºC	$20 \times [4 + 1]$	4:1	0.24	16.3 nm	1.72
H9A1	300 ºC	$10 \times [9 + 1]$	9:1	0.11	15.4 nm	1.34
H9A1	400 ºC	$10 \times [9 + 1]$	9:1	0.14	21.4 nm	1.84

Table I. List of films subjected to electrical measurements, grown with HfO_2:Al_2O_3 cycle sequences indicated, on TiN substrates. Al:Hf atomic ratios were estimated by XRF. The thickness and refractive index, n, values indicated were measured by spectroscopic ellipsometry. The refractive index is given for the wavelength of 633 nm. The code used to name the samples references the number of cycles for each oxide HfO_2 (H) and Al_2O_3 (A) in that order.

In order to determine the films thicknesses, optical measurements were performed on a spectroscopic ellipsometer GES-5E (Semilab Co), applying Tauc-Lorentz dispersion law. Elemental composition of the films was measured by wave dispersive X-ray fluorescence spectroscopy (XRF) with Rigaku ZSX-400. The lattice ordering was evaluated by grazing incidence X-ray diffractometry (GIXRD), using a X-ray diffractometer Smart-Lab Rigaku with CuKα radiation.

Resistive switching measurements were carried out by means of a semiconductor analyzer (Keithley 4200SCS), with samples put on a light-tight probe station. DC voltage was applied to the top electrode, while the bottom one remained grounded. Characteristic ReRAM current-voltage (I-V) curves were measured by applying voltage sweeps. Memory maps were obtained by applying incremental voltage pulses (programming voltage) while measuring the current at a constant reading voltage of 0.1 V [14]. Small signal measurements were carried out by applying a 30 mV signal at 100 kHz over the DC voltage.

3. Results and discussion

The HfO_2:Al_2O_3 films grown in the present study remained essentially amorphous, as revealed by GIXRD measurements,
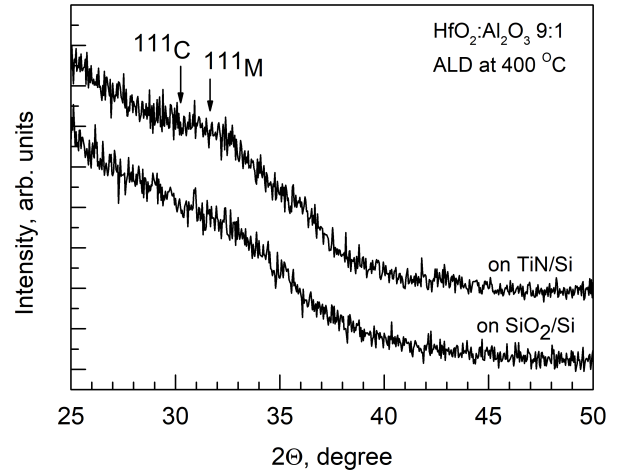

Figure 1: GIXRD Grazing incidence diffraction patterns of 15-22 nm thick amorphous HfO_2:Al_2O_3 films grown at 400 ºC on TiN and reference SiO_2/Si substrate surfaces. Locations of the most intense 111 reflections, if apparent, from cubic, C, and monoclinic, M, phases of HfO_2, in accord with powder diffraction databases, are denoted by corresponding Miller indexes.

regardless of the HfO_2:Al_2O_3 cycle ratio. Partially, the amorphicity was due to the low thickness of the films. The 15-22 nm thick films grown with cycle ratio of 9:1 at temperatures as high as 400 ºC on TiN may have exhibited very weak tendency to crystallize (Fig. 1). The tendency was further proven by growing reference films at 400 ºC, using the same cycle ratio, to thicknesses around 70 nm. In the latter films, strong reflections at 31, 36, 52 and 62 degrees were detected (not shown), indicating the stabilization of markedly deformed cubic phase of HfO_2. Thus, one can not rule out some short range ordering in 20 nm thick HfO_2:Al_2O_3 films. H9A1 films grown at 400ºC could also be densified in comparison to those grown at 300 ºC, as implied by the relatively higher refractive index measured by ellipsometry (Table I).

The thin film stacks examined demonstrated well defined resistive switching characteristics. Under certain electrical stimulus, the resistance changed and retained its value with no power consumption (non-volatile effect), due to the creation of a conductive filament between the top and bottom metals. All the films required an electroforming process (formation of the CF for the first time) after which the typical resistive switching I-V curves were measured (Fig. 2-a). The samples showed appreciable repetitiveness and functional windows between high and low resistance states (HRS and LRS). The samples grown with cycle ratios 1:1 (H1A1) and 9:1 (H9A1) possessed almost the same commutation voltages, but the H9A1 sample demonstrated lower current values in both high and low resistance states. The film grown with cycle ratio of 4:1 (H4A1) differed from the rest of the samples by increased set and reset voltages, as well as by the highest HRS and lowest LRS currents. This observation is supported by the memory maps that can be seen in Fig. 2-b.

These results might be explained by taking into account the multilayer-like structure in each film. As the conductive filament between both metal electrodes is supposedly formed by
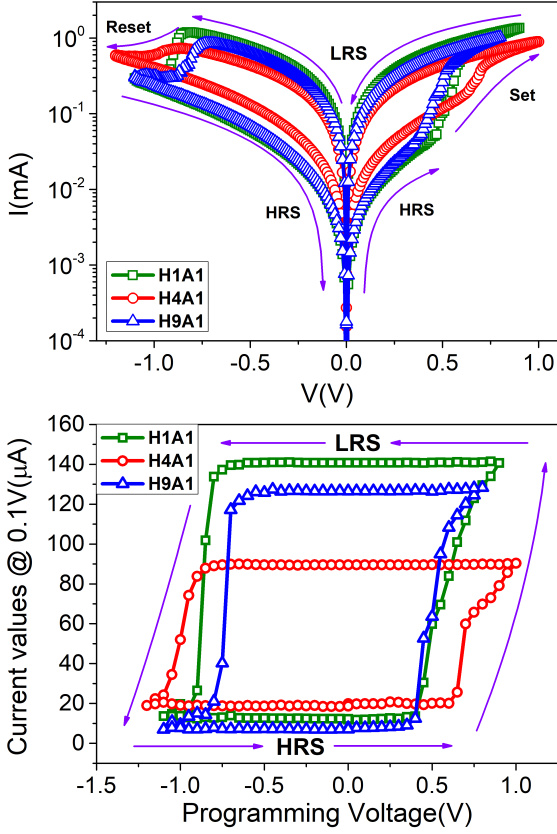
Figure 2: a - Current-voltage (I-V) loops of the different HfO$_2$:Al$_2$O$_3$ samples grown at 300°C. The curves presented are the average of 20 I-V cycles for each sample. b - Memory maps of the HfO$_2$:Al$_2$O$_3$ samples.
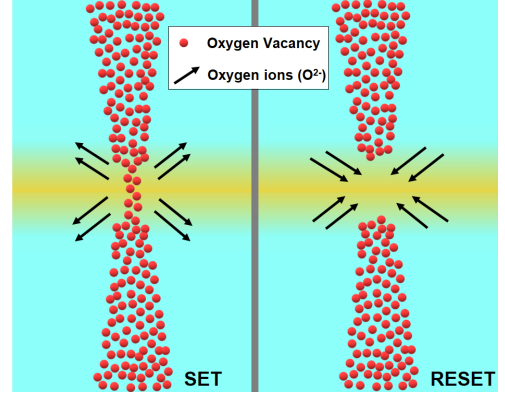

Figure 3: Schematics of the proposed RS mechanism in the HfO$_2$:Al$_2$O$_3$ films grown with cycle ratios of 9:1 (H9A1) and 4:1 (H4A1).

anion (oxygen) vacancies [15, 16], we must consider different reactivities for each oxide. Previously it has been already considered that one Al$_2$O$_3$ ALD cycle does not suffice for the formation of a continuous thin Al$_2$O$_3$ layer, and the result is most likely a diffuse HfAlO$_x$ layer. Nonetheless, aluminium must be oxidized, because it is grown via oxidation. Due to the fact that the aluminium oxide is less likely to be reduced, oxygen ions may recombine with oxygen vacancies in these layers, leading to the breaking of the filament. This can be supported by the results presented by Fadida et al. [17] in a study devoted to the high-permittivity oxides, which indicated a difference between HfO$_2$ and HfAlO$_x$ binding energies that is mainly due to the higher Al-O energy compared to that of Hf-O. This is also consistent with the fact that the first ionization energy of aluminium is lower than that of hafnium, as the aluminium atom has a single electron in its outer shell (electronic configuration of Al: [Ne] 3s2 3p1). Moreover, previous works on resistively switching oxide stacks have demonstrated that an asymmetric filament forms between different dielectrics constituting the switching medium, leading to the weakening of the filament at the interface of neighbouring dielectrics [4, 8, 18, 19]. As our HfAlO$_x$ layer thickness is hardly determined after only one ALD cycle, it is possible that the breaking of the filament occurs not only at the interfaces between HfO$_2$ and HfAlO$_x$, but within the diffuse HfAlO$_x$ layer thickness. Thus, the filament formation may

be controlled by the separation of the HfAlO$_x$ layers. The proposed resistive switching mechanism of our samples is depicted in Fig. 3.

In the case of the HfO$_2$:Al$_2$O$_3$ film grown with cycle ratio 1:1 (sample H1A1), our schematics, proposed for other samples with spatially more separated HfAlO$_x$ layers, does not apply, as there are no periodical changes in composition throughout the dielectric, whereas the dielectric itself is composed of HfAlO$_x$. However, it came out that the switching behaviour was fairly similar to that in the H9A1 sample. It is worth noting that the currents in the LRS remained higher in the sample H1A1 compared to those in the sample H9A1. This was indicative of the higher density of structural defects in the sample H1A1 and thus, higher leakage currents. Hence, application of periodical multilayers would evidently be advantageous when aiming at switching structures providing lower power consumption. Complementarily, the small signal measurements were carried out to record conductance behaviour against switching voltage, and the results (Fig. 4) confirmed insulation properties better defined in the film containing multiple HfO$_2$/HfAlO$_x$ barriers to the conduction channels, further confirming our hypothesis on the RS mechanism.
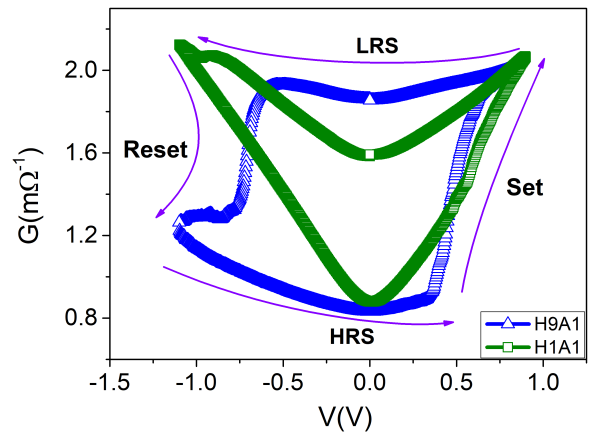

Figure 4: Conductance-voltage (G-V) loops averaged for the H1A1 and H9A1 samples grown at 300°C.

3

Tendency to the crystallization (mentioned in the first paragraph of this section) in the distinct HfO_2 intermediate layers may not usefully influence the LRS:HRS ratio. Comparing the $HfO_2:Al_2O_3$ film grown with cycle ratio of 9:1 at 300 and 400 ºC, one can see that the currents in high resistance state have increased in the film grown at higher temperature (Fig. 5). Although long-range ordering was not possible in these samples, short-range ordering was probable and may explain the conductivity increased in the sample grown at higher temperature. It can also be seen that the LRS hardly differs in both samples, which could be justified by the fact that the filament was the main conduction mechanism in this state.

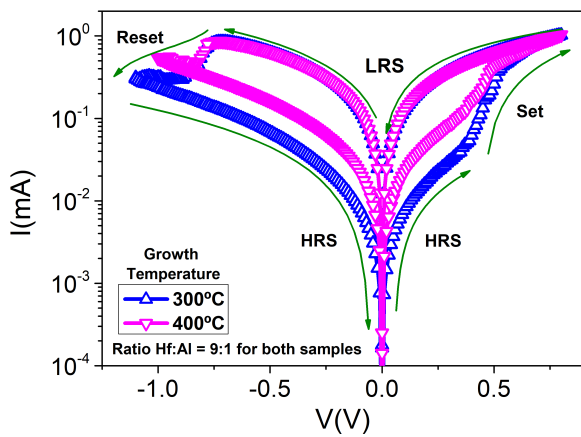Figure 5: Average I-V loops of the H9A1 samples grown at different temperatures indicated by labels.

4. Summary and conclusions

$HfO_2:HfAlO_x$ films grown by ALD using $HfO_2:Al_2O_3$ cycle ratios of 1:1 and 9:1 demonstrated wide functional ratios between low and high resistance states together with abrupt set and reset processes. Lower current values measured in both low and high resistance states, as well as more defined insulator properties, made the multilayered film grown with cycle ratio 9:1 more appropriate for possible memory applications. At the same time, a film grown with cycle ratio of 4:1 showed the narrowest window between both resistance states, with higher commutation voltages. A resistive switching mechanism is proposed where the HfO_2 intermediate layers contribute to the exploitation of oxygen vacancies along conductive paths formed in the switching medium, while spacer $HfAlO_x$ layers, although defective, may allow efficient control of the filament formation and disruption. Avoiding crystallization in such structures could procure resistively switching media exhibiting lower current values for the high resistance state.

References

[1] A. C. Jasmin, Filamentary model in resistive switching materials, in: AIP Conference Proceedings, volume 1901, AIP Publishing LLC, 2017, p. 060004.

[2] F. Zahoor, T. Z. Azni Zulkifli, F. A. Khanday, Resistive random access memory (RRAM): an overview of materials, switching mechanism, performance, multilevel cell (MLC) storage, modeling, and applications, Nanoscale research letters 15 (2020) 1–26.

[3] J. Niinistö, K. Kukli, M. Heikkilä, M. Ritala, M. Leskelä, Atomic layer deposition of high-k oxides of the group 4 metals for memory applications, Advanced Engineering Materials 11 (2009) 223–234.

[4] L.-G. Wang, X. Qian, Y.-Q. Cao, Z.-Y. Cao, G.-Y. Fang, A.-D. Li, D. Wu, Excellent resistive switching properties of atomic layer-deposited $Al_2O_3/HfO_2/Al_2O_3$ trilayer structures for non-volatile memory applications, Nanoscale research letters 10 (2015) 1–8.

[5] M. Cazorla, S. Aldana, M. Maestro, M. B. González, F. Campabadal, E. Moreno, F. Jiménez-Molinos, J. B. Roldán, Thermal study of multilayer resistive random access memories based on HfO_2 and Al_2O_3 oxides, Journal of Vacuum Science & Technology B, Nanotechnology and Microelectronics: Materials, Processing, Measurement, and Phenomena 37 (2019) 012204.

[6] M. Mallol, M. Gonzalez, F. Campabadal, Impact of the HfO_2/Al_2O_3 stacking order on unipolar RRAM devices, Microelectronic Engineering 178 (2017) 168–172.

[7] M. Maestro-Izquierdo, M. Gonzalez, F. Jimenez-Molinos, E. Moreno, J. Roldan, F. Campabadal, Unipolar resistive switching behavior in $Al_2O_3HfO_2$ multilayer dielectric stacks: fabrication, characterization and simulation, Nanotechnology 31 (2020) 135202.

[8] C. Mahata, M. Kang, S. Kim, Multi-level analog resistive switching characteristics in tri-layer $HfO_2/Al_2O_3/HfO_2$ based memristor on ITO electrode, Nanomaterials 10 (2020) 2069.

[9] A. S. Sokolov, S. K. Son, D. Lim, H. H. Han, Y.-R. Jeon, J. H. Lee, C. Choi, Comparative study of Al_2O_3, HfO_2, and $HfAlO_x$ for improved self-compliance bipolar resistive switching, Journal of the American Ceramic Society 100 (2017) 5638–5648.

[10] A. Markeev, A. Chouprik, K. Egorov, Y. Lebedinskii, A. Zenkevich, O. Orlov, Multilevel resistive switching in ternary $Hf_xAl_{1-x}O_y$ oxide with graded Al depth profile, Microelectronic engineering 109 (2013) 342–345.

[11] W.-H. Tzeng, C.-W. Zhong, K.-C. Liu, K.-M. Chang, H.-C. Lin, Y.-C. Chan, C.-C. Kuo, F.-Y. Tsai, M. H. Tseng, P.-S. Chen, et al., Resistive switching characteristics of multilayered (HfO_2/Al_2O_3) nn= 19 thin film, Thin solid films 520 (2012) 3415–3418.

[12] X. Huang, H. Wu, B. Gao, D. C. Sekar, L. Dai, M. Kellam, G. Bronner, N. Deng, H. Qian, HfO_2/Al_2O_3 multilayer for RRAM arrays: a technique to improve tail-bit retention, Nanotechnology 27 (2016) 395201.

[13] S. Brivio, J. Frascaroli, S. Spiga, Role of al doping in the filament disruption in HfO_2 resistance switches, Nanotechnology 28 (2017) 395202.

[14] S. Dueñas, H. Castán, K. Kukli, M. Mikkor, K. Kalam, T. Arroval, A. Tamm, Memory maps: reading rram devices without power consumption, ECS transactions 85 (2018) 201.

[15] T.-C. Chang, K.-C. Chang, T.-M. Tsai, T.-J. Chu, S. M. Sze, Resistance random access memory, Materials Today 19 (2016) 254–264.

[16] S. Munjal, N. Khare, Advances in resistive switching based memory devices, Journal of Physics D: Applied Physics 52 (2019) 433002.

[17] S. Fadida, F. Palumbo, L. Nyns, D. Lin, S. Van Elshocht, M. Caymax, M. Eizenberg, Hf-based high-k dielectrics for p-Ge mos gate stacks, Journal of Vacuum Science & Technology B, Nanotechnology and Microelectronics: Materials, Processing, Measurement, and Phenomena 32 (2014) 03D105.

[18] C.-Y. Huang, C.-Y. Huang, T.-L. Tsai, C.-A. Lin, T.-Y. Tseng, Switching mechanism of double forming process phenomenon in ZrO_x/HfO_y bilayer resistive switching memory structure with large endurance, Applied Physics Letters 104 (2014) 062901.

[19] T.-L. Tsai, H.-Y. Chang, J. J.-C. Lou, T.-Y. Tseng, A high performance transparent resistive switching memory made from $ZrO_2/AlON$ bilayer structure, Applied Physics Letters 108 (2016) 153505.

Author Biography

Salvador Dueñas was born in Spain in 1961. He received the Bachelor and Ph.D. degrees in Physics from the University of Valladolid, Valladolid, Spain, in 1984 and 1989, respectively. In1984, he joined the Department of Electronics, University of Valladolid, where he was an as Assistant Professor, became Associate Professor in 1987, and a Professor in 2010. His current research interests include high-k dielectrics, solar cells, defects in semiconductors, and electrical characterization of electronic materials and devices. He is author of more than 270 scientific publications. He was General Director of the Scientific Park of the University of Valladolid from 2010 to 2014, and General Manager of Research Projects on Electronic and Communication Technologies of the Science and Innovation Research Ministry of the Spanish Government from 2007 to 2010. Currently, he coordinates the Recognized Research Group " Electrical Characterization of Electronic Materials and Devices" of the University of Valladolid.

The main objective of our research group is the adaptation and fine-tuning to structures of a set of standard techniques based on the analysis of conduction mechanisms and electrical parameters (capacity, conductance, etc.). In addition, we have developed and extensively used original techniques and new variants of these standard techniques that are more precise and appropriate in certain circumstances.

Our scientific interest has focused in recent years on the study of high permittivity dielectrics in a double aspect: on the one hand, in the search for an alternative material to silicon dioxide as a gate insulator for integrated circuit transistors; on the other hand, in the development of applications in the field of memories, specifically those based on the resistive switching and ferroelectricity phenomena. Another point of interest for us is the use of graphene layers in combination con functional oxides layers.

Declaration of interests

☒The authors declare that they have no known competing financial interests or personal relationships that could have appeared to influence the work reported in this paper.

☐The authors declare the following financial interests/personal relationships which may be considered as potential competing interests:

Effective control of filament efficiency by means of spacer HfAlO$_x$ layers and growth temperature in HfO$_2$ based ReRAM devices

G. Vinuesa[a], Ó. G. Ossorio[a], H. García[a], B. Sahelices[a], H. Castán[a], S. Dueñas[a,*], M. Kull[b], A. Tarre[b], T. Jõgiaas[b], A. Tamm[b], A. Kasikov[b], K. Kukli[b]

[a]*Department of Electronics, University of Valladolid, Paseo de Belén 15, Valladolid, E-47011, Spain*
[b]*Institute of Physics, University of Tartu, W. Ostwald 1, Tartu, 50411, Estonia*

Abstract

Resistive switching random access memories are being thoroughly studied as prospective non-volatile memories. In this paper, we report electrical characterization of HfO$_2$-Al$_2$O$_3$ based metal-insulator-metal structures devised using atomic layer deposition. Dependences of electrical behavior on HfO$_2$:Al$_2$O$_3$ cycle ratio is studied. An explanation for the differences between the Resistive Switching properties of the samples is proposed, based on the distribution of HfAlO$_x$ layers of the sample. Dependence of the RS properties of the samples on their growth temperature is discussed.

Keywords: RRAM, NVM, MIM stack, resistive switching, hafnium oxide, aluminium oxide, alumina, hafnium-aluminum oxide

1. Introduction

Non-volatile memory devices based on the resistive switching (RS) effect are considered as the most promising technology for future memory applications due to their excellent characteristics, such as good dimensional scalability and small operating voltages. The RS effect is based in the growth of conductive filaments (CF) in the dielectric film mounted between metal electrodes under a voltage applied to the electrodes [1, 2]. While HfO$_2$ is one of the most widely studied dielectrics for the fabrication of ReRAM devices [3], alternately layered nanomaterials are of increasing interest [4], as screening of the most appropriate combinations of materials for the dielectric layer is one of the issues in ReRAM fabrication.

In several previously conducted works, HfO$_2$-Al$_2$O$_3$ films have demonstrated advanced RS characteristics in comparison with both single HfO$_2$ and Al$_2$O$_3$ films. Resistive switching behavior has been evaluated in Al$_2$O$_3$/HfO$_2$ bilayer [5, 6, 7], Al$_2$O$_3$/HfO$_2$/Al$_2$O$_3$ trilayer [4, 7], and pentalayer [7] structures ALD-grown at 225 - 250 ºC with total thicknesses reaching 20 nm. In another study, Al$_2$O$_3$/HfO$_2$/Al$_2$O$_3$ trilayers grown at 150 ºC with thicknesses of 12 nm were able to demonstrate multilevel switching characteristics [8]. Periodical HfO$_2$-Al$_2$O$_3$ multilayers containing equal amounts of Hf and Al have been grown to a thickness of 6.5 nm at 250 ºC [9]. However, in this latter study the thickness of the constituent layers was not revealed. Hf$_x$Al$_{1-x}$O$_y$ films have been grown at 240 ºC with graded profile whereby the HfO$_2$:Al$_2$O$_3$ ALD cycle ratio was varied from 9:1 to 1:4 [10]. Another study indicated that 30 nm thick nanolaminates of HfO$_2$-Al$_2$O$_3$ bilayers composed of 1.2 nm thick HfO$_2$ and 0.2 nm thick Al$_2$O$_3$ layers could be grown at temperatures as low as 100 ºC [11].

The application of 3 consecutive HfO$_2$ ALD cycles alternately with 2 Al$_2$O$_3$ cycles has enabled the deposition of RS-behaving HfO$_2$-Al$_2$O$_3$ multilayers at 200 ºC with total thicknesses of 8 nm, showing an improvement in the High Resistance State (HRS) retention characteristics when compared with HfO$_2$-only films [12]. In the latter study, however, the precursor chemistry was not revealed. Apparently, contradicting results were obtained in a study, where HfO$_2$ films doped with 7 at.% Al were grown using HfO$_2$:Al$_2$O$_3$ ALD cycle ratio of 12:1 to the thickness of 5-6 nm from Al(CH$_3$)$_3$, (MeCp)2Hf(Me)(OMe) and H$_2$O at 300 ºC [13]. In the latter study, filament disruption was, as proposed, suppressed by the defects introduced by Al$_2$O$_3$ as the high resistance state was stabilized at higher currents. Most commonly, the metal precursors exploited in ALD of resistively switching stacks consisting of HfO$_2$ and Al$_2$O$_3$ have been Hf[N(C$_2$H$_5$)CH$_3$]$_4$ (TEMAHf), and Al(CH$_3$)$_3$ (TMA), whereby H$_2$O served as oxygen precursor [4, 5, 6, 7, 8, 9, 10, 11].

The present study is devoted to the resistive switching properties of HfO$_2$-Al$_2$O$_3$ multilayers, whereby the films were grown by ALD to thicknesses of 10-15 nm at different temperatures of 300 ºC and 400 ºC from TEMAHf, TMA, and O$_2$ plasma. Examination of differences in the properties of the selected films grown using different periodicity of constituent oxides and at different growth temperatures was of importance.

2. Experimental details

Atomic layer deposition of HfO$_2$–Al$_2$O$_3$ multilayer films was carried out using TEMAHf, TMA and remote O$_2$ plasma in a commercial Picosun TM R-200 Advanced ALD system.

TEMAHf and TMA were evaporated at 100ºC and 22 ºC, respectively. The amorphous films were grown on TiN/Si substrates by changing the $HfO_2:Al_2O_3$ cycle ratio between 1:1 and 9:1 with a total amount of 100 ALD cycles to the thickness of 12-16 nm, somewhat influenced by the cycle ratios. All the samples were supplied by top Ti electrodes with an area of 0.052 mm^2, by electron-beam evaporation through shadow mask at room temperature. Since a single ALD cycle of Al_2O_3 can, plausibly, not result in the formation of a full oxide monolayer, the solid multilayers grown in such experiments may also be regarded as HfO_2 films deposited alternately with somewhat diffuse $HfAlO_x$ barrier layers (which can be referred to as spacer layers). The host HfO_2 films were grown using ALD cycle sequence of 0.3-4.0-15.0-4.0 seconds for TEMAHf pulse-purge-O_2 plasma pulse-purge times respectively. The intermediate Al_2O_3 cycle followed a sequence of 0.1-4.0-15.0-4.0 seconds applied for TMA pulse-purge-O_2 plasma pulse-purge times. Sample series with $HfO_2:Al_2O_3$ cycle ratios 1:1, 4:1 and 9:1 was grown at 300ºC, completed with a film grown with the cycle ratio of 9:1 at 400 ºC. The list of samples with their respective characteristics can be found in Table. I.

Sample	T_{GROWTH}	Cycle Sequence	$HfO_2:Al_2O_3$ cycle ratio	Al:Hf ratio	Thickness	n
H1A1	300 ºC	$50 \times [1+1]$	1:1	0.96	19.2 nm	1.49
H4A1	300 ºC	$20 \times [4+1]$	4:1	0.24	16.3 nm	1.72
H9A1	300 ºC	$10 \times [9+1]$	9:1	0.11	15.4 nm	1.34
H9A1	400 ºC	$10 \times [9+1]$	9:1	0.14	21.4 nm	1.84

Table I. List of films subjected to electrical measurements, grown with $HfO_2:Al_2O_3$ cycle sequences indicated, on TiN substrates. Al:Hf atomic ratios were estimated by XRF. The thickness and refractive index, n, values indicated were measured by spectroscopic ellipsometry. The refractive index is given for the wavelength of 633 nm. The code used to name the samples references the number of cycles for each oxide HfO_2 (H) and Al_2O_3 (A) in that order.

In order to determine the films thicknesses, optical measurements were performed on a spectroscopic ellipsometer GES-5E (Semilab Co), applying Tauc-Lorentz dispersion law. Elemental composition of the films was measured by wave dispersive X-ray fluorescence spectroscopy (XRF) with Rigaku ZSX-400. The lattice ordering was evaluated by grazing incidence X-ray diffractometry (GIXRD), using a X-ray diffractometer Smart-Lab Rigaku with CuKα radiation.

Resistive switching measurements were carried out by means of a semiconductor analyzer (Keithley 4200SCS), with samples put on a light-tight probe station. DC voltage was applied to the top electrode, while the bottom one remained grounded. Characteristic ReRAM current-voltage (I-V) curves were measured by applying voltage sweeps. Memory maps were obtained by applying incremental voltage pulses (programming voltage) while measuring the current at a constant reading voltage of 0.1 V [14]. Small signal measurements were carried out by applying a 30 mV signal at 100 kHz over the DC voltage.

3. Results and discussion

The $HfO_2:Al_2O_3$ films grown in the present study remained essentially amorphous, as revealed by GIXRD measurements,
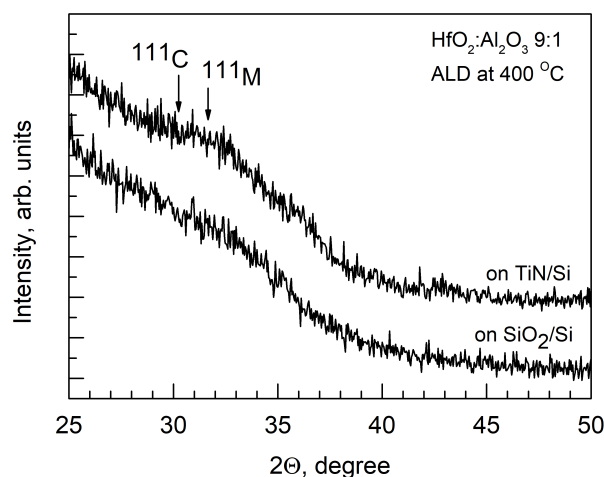

Figure 1: GIXRD Grazing incidence diffraction patterns of 15-22 nm thick amorphous $HfO_2:Al_2O_3$ films grown at 400 ºC on TiN and reference SiO_2/Si substrate surfaces. Locations of the most intense 111 reflections, if apparent, from cubic, C, and monoclinic, M, phases of HfO_2, in accord with powder diffraction databases, are denoted by corresponding Miller indexes.

regardless of the $HfO_2:Al_2O_3$ cycle ratio. Partially, the amorphicity was due to the low thickness of the films. The 15-22 nm thick films grown with cycle ratio of 9:1 at temperatures as high as 400 ºC on TiN may have exhibited very weak tendency to crystallize (Fig. 1). The tendency was further proven by growing reference films at 400 ºC, using the same cycle ratio, to thicknesses around 70 nm. In the latter films, strong reflections at 31, 36, 52 and 62 degrees were detected (not shown), indicating the stabilization of markedly deformed cubic phase of HfO_2. Thus, one can not rule out some short range ordering in 20 nm thick $HfO_2:Al_2O_3$ films. H9A1 films grown at 400ºC could also be densified in comparison to those grown at 300 ºC, as implied by the relatively higher refractive index measured by ellipsometry (Table I).

The thin film stacks examined demonstrated well defined resistive switching characteristics. Under certain electrical stimulus, the resistance changed and retained its value with no power consumption (non-volatile effect), due to the creation of a conductive filament between the top and bottom metals. All the films required an electroforming process (formation of the CF for the first time) after which the typical resistive switching I-V curves were measured (Fig. 2-a). The samples showed appreciable repetitiveness and functional windows between high and low resistance states (HRS and LRS). The samples grown with cycle ratios 1:1 (H1A1) and 9:1 (H9A1) possessed almost the same commutation voltages, but the H9A1 sample demonstrated lower current values in both high and low resistance states. The film grown with cycle ratio of 4:1 (H4A1) differed from the rest of the samples by increased set and reset voltages, as well as by the highest HRS and lowest LRS currents. This observation is supported by the memory maps that can be seen in Fig. 2-b.

These results might be explained by taking into account the multilayer-like structure in each film. As the conductive filament between both metal electrodes is supposedly formed by
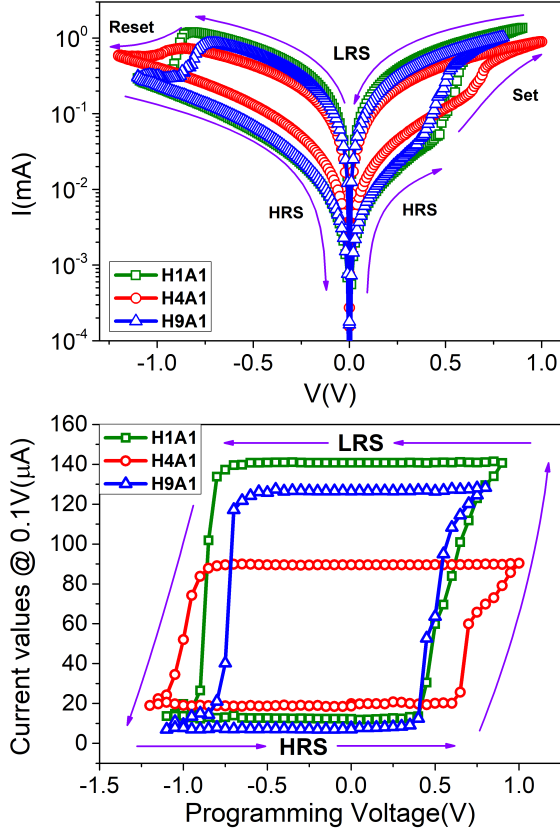
Figure 2: a - Current-voltage (I-V) loops of the different HfO$_2$:Al$_2$O$_3$ samples grown at 300ºC. The curves presented are the average of 20 I-V cycles for each sample. b - Memory maps of the HfO$_2$:Al$_2$O$_3$ samples.
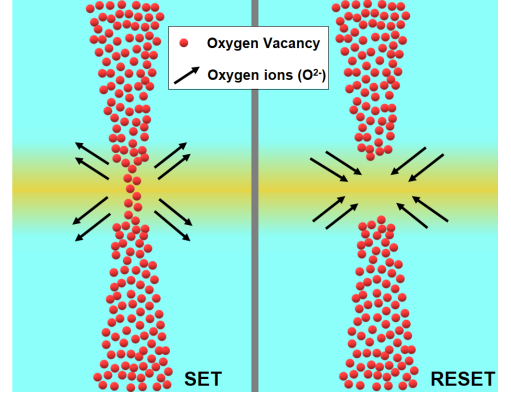

Figure 3: Schematics of the proposed RS mechanism in the HfO$_2$:Al$_2$O$_3$ films grown with cycle ratios of 9:1 (H9A1) and 4:1 (H4A1).

be controlled by the separation of the HfAlO$_x$ layers. The proposed resistive switching mechanism of our samples is depicted in Fig. 3.

In the case of the HfO$_2$:Al$_2$O$_3$ film grown with cycle ratio 1:1 (sample H1A1), our schematics, proposed for other samples with spatially more separated HfAlO$_x$ layers, does not apply, as there are no periodical changes in composition throughout the dielectric, whereas the dielectric itself is composed of HfAlO$_x$. However, it came out that the switching behaviour was fairly similar to that in the H9A1 sample. It is worth noting that the currents in the LRS remained higher in the sample H1A1 compared to those in the sample H9A1. This was indicative of the higher density of structural defects in the sample H1A1 and thus, higher leakage currents. Hence, application of periodical multilayers would evidently be advantageous when aiming at switching structures providing lower power consumption. Complementarily, the small signal measurements were carried out to record conductance behaviour against switching voltage, and the results (Fig. 4) confirmed insulation properties better defined in the film containing multiple HfO$_2$/HfAlO$_x$ barriers to the conduction channels, further confirming our hypothesis on the RS mechanism.

anion (oxygen) vacancies [15, 16], we must consider different reactivities for each oxide. Previously it has been already considered that one Al$_2$O$_3$ ALD cycle does not suffice for the formation of a continuous thin Al$_2$O$_3$ layer, and the result is most likely a diffuse HfAlO$_x$ layer. Nonetheless, aluminium must be oxidized, because it is grown via oxidation. Due to the fact that the aluminium oxide is less likely to be reduced, oxygen ions may recombine with oxygen vacancies in these layers, leading to the breaking of the filament. This can be supported by the results presented by Fadida et al. [17] in a study devoted to the high-permittivity oxides, which indicated a difference between HfO$_2$ and HfAlO$_x$ binding energies that is mainly due to the higher Al-O energy compared to that of Hf-O. This is also consistent with the fact that the first ionization energy of aluminium is lower than that of hafnium, as the aluminium atom has a single electron in its outer shell (electronic configuration of Al: [Ne] 3s2 3p1). Moreover, previous works on resistively switching oxide stacks have demonstrated that an asymmetric filament forms between different dielectrics constituting the switching medium, leading to the weakening of the filament at the interface of neighbouring dielectrics [4, 8, 18, 19]. As our HfAlO$_x$ layer thickness is hardly determined after only one ALD cycle, it is possible that the breaking of the filament occurs not only at the interfaces between HfO$_2$ and HfAlO$_x$, but within the diffuse HfAlO$_x$ layer thickness. Thus, the filament formation may
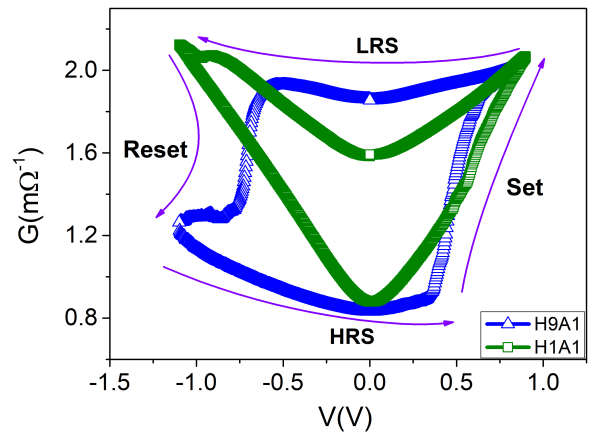

Figure 4: Conductance-voltage (G-V) loops averaged for the H1A1 and H9A1 samples grown at 300ºC.

Tendency to the crystallization (mentioned in the first paragraph of this section) in the distinct HfO$_2$ intermediate layers may not usefully influence the LRS:HRS ratio. Comparing the HfO$_2$:Al$_2$O$_3$ film grown with cycle ratio of 9:1 at 300 and 400 ºC, one can see that the currents in high resistance state have increased in the film grown at higher temperature (Fig. 5). Although long-range ordering was not possible in these samples, short-range ordering was probable and may explain the conductivity increased in the sample grown at higher temperature. It can also be seen that the LRS hardly differs in both samples, which could be justified by the fact that the filament was the main conduction mechanism in this state.
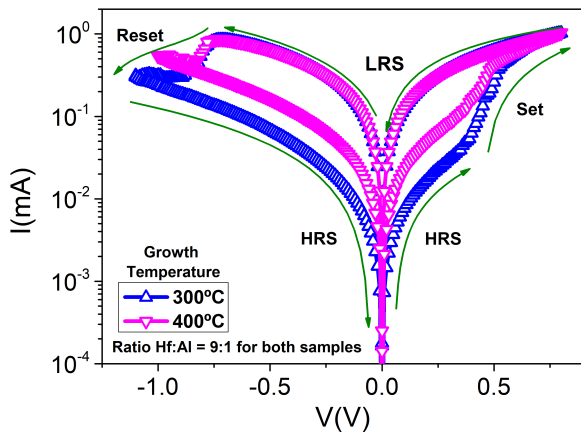

Figure 5: Average I-V loops of the H9A1 samples grown at different temperatures indicated by labels.

4. Summary and conclusions

HfO$_2$:HfAlO$_x$ films grown by ALD using HfO$_2$:Al$_2$O$_3$ cycle ratios of 1:1 and 9:1 demonstrated wide functional ratios between low and high resistance states together with abrupt set and reset processes. Lower current values measured in both low and high resistance states, as well as more defined insulator properties, made the multilayered film grown with cycle ratio 9:1 more appropriate for possible memory applications. At the same time, a film grown with cycle ratio of 4:1 showed the narrowest window between both resistance states, with higher commutation voltages. A resistive switching mechanism is proposed where the HfO$_2$ intermediate layers contribute to the exploitation of oxygen vacancies along conductive paths formed in the switching medium, while spacer HfAlO$_x$ layers, although defective, may allow efficient control of the filament formation and disruption. Avoiding crystallization in such structures could procure resistively switching media exhibiting lower current values for the high resistance state.

Acknowledgements

References

[1] A. C. Jasmin, Filamentary model in resistive switching materials, in: AIP Conference Proceedings, volume 1901, AIP Publishing LLC, 2017, p. 060004.

[2] F. Zahoor, T. Z. Azni Zulkifli, F. A. Khanday, Resistive random access memory (RRAM): an overview of materials, switching mechanism, performance, multilevel cell (MLC) storage, modeling, and applications, Nanoscale research letters 15 (2020) 1–26.

[3] J. Niinistö, K. Kukli, M. Heikkilä, M. Ritala, M. Leskelä, Atomic layer deposition of high-k oxides of the group 4 metals for memory applications, Advanced Engineering Materials 11 (2009) 223–234.

[4] L.-G. Wang, X. Qian, Y.-Q. Cao, Z.-Y. Cao, G.-Y. Fang, A.-D. Li, D. Wu, Excellent resistive switching properties of atomic layer-deposited Al$_2$O$_3$/HfO$_2$/Al$_2$O$_3$ trilayer structures for non-volatile memory applications, Nanoscale research letters 10 (2015) 1–8.

[5] M. Cazorla, S. Aldana, M. Maestro, M. B. González, F. Campabadal, E. Moreno, F. Jiménez-Molinos, J. B. Roldán, Thermal study of multilayer resistive random access memories based on HfO$_2$ and Al$_2$O$_3$ oxides, Journal of Vacuum Science & Technology B, Nanotechnology and Microelectronics: Materials, Processing, Measurement, and Phenomena 37 (2019) 012204.

[6] M. Mallol, M. Gonzalez, F. Campabadal, Impact of the HfO$_2$/Al$_2$O$_3$ stacking order on unipolar RRAM devices, Microelectronic Engineering 178 (2017) 168–172.

[7] M. Maestro-Izquierdo, M. Gonzalez, F. Jimenez-Molinos, E. Moreno, J. Roldan, F. Campabadal, Unipolar resistive switching behavior in Al$_2$O$_3$HfO$_2$ multilayer dielectric stacks: fabrication, characterization and simulation, Nanotechnology 31 (2020) 135202.

[8] C. Mahata, M. Kang, S. Kim, Multi-level analog resistive switching characteristics in tri-layer HfO$_2$/Al$_2$O$_3$/HfO$_2$ based memristor on ITO electrode, Nanomaterials 10 (2020) 2069.

[9] A. S. Sokolov, S. K. Son, D. Lim, H. H. Han, Y.-R. Jeon, J. H. Lee, C. Choi, Comparative study of Al$_2$O$_3$, HfO$_2$, and HfAlO$_x$ for improved self-compliance bipolar resistive switching, Journal of the American Ceramic Society 100 (2017) 5638–5648.

[10] A. Markeev, A. Chouprik, K. Egorov, Y. Lebedinskii, A. Zenkevich, O. Orlov, Multilevel resistive switching in ternary Hf$_x$Al$_{1-x}$O$_y$ oxide with graded Al depth profile, Microelectronic engineering 109 (2013) 342–345.

[11] W.-H. Tzeng, C.-W. Zhong, K.-C. Liu, K.-M. Chang, H.-C. Lin, Y.-C. Chan, C.-C. Kuo, F.-Y. Tsai, M. H. Tseng, P.-S. Chen, et al., Resistive switching characteristics of multilayered (HfO$_2$/Al$_2$O$_3$) nn= 19 thin film, Thin solid films 520 (2012) 3415–3418.

[12] X. Huang, H. Wu, B. Gao, D. C. Sekar, L. Dai, M. Kellam, G. Bronner, N. Deng, H. Qian, HfO$_2$/Al$_2$O$_3$ multilayer for RRAM arrays: a technique to improve tail-bit retention, Nanotechnology 27 (2016) 395201.

[13] S. Brivio, J. Frascaroli, S. Spiga, Role of al doping in the filament disruption in HfO$_2$ resistance switches, Nanotechnology 28 (2017) 395202.

[14] S. Dueñas, H. Castán, K. Kukli, M. Mikkor, K. Kalam, T. Arroval, A. Tamm, Memory maps: reading rram devices without power consumption, ECS transactions 85 (2018) 201.

[15] T.-C. Chang, K.-C. Chang, T.-M. Tsai, T.-J. Chu, S. M. Sze, Resistance random access memory, Materials Today 19 (2016) 254–264.

[16] S. Munjal, N. Khare, Advances in resistive switching based memory devices, Journal of Physics D: Applied Physics 52 (2019) 433002.

[17] S. Fadida, F. Palumbo, L. Nyns, D. Lin, S. Van Elshocht, M. Caymax, M. Eizenberg, Hf-based high-k dielectrics for p-Ge mos gate stacks, Journal of Vacuum Science & Technology B, Nanotechnology and Microelectronics: Materials, Processing, Measurement, and Phenomena 32 (2014) 03D105.

[18] C.-Y. Huang, C.-Y. Huang, T.-L. Tsai, C.-A. Lin, T.-Y. Tseng, Switching mechanism of double forming process phenomenon in ZrO$_x$/HfO$_y$ bilayer resistive switching memory structure with large endurance, Applied Physics Letters 104 (2014) 062901.

[19] T.-L. Tsai, H.-Y. Chang, J. J.-C. Lou, T.-Y. Tseng, A high performance transparent resistive switching memory made from ZrO$_2$/AlON bilayer structure, Applied Physics Letters 108 (2016) 153505.